Simplified integrative simulation of short fibre reinforced polymers under varying thermal conditions

Christian Witzgall[1], Sandro Wartzack[1]

[1]Chair of Engineering Design KTmfk
University of Erlangen-Nuremberg FAU, Germany

1 Introduction

Short fibre reinforced polymers (SFRPs) are increasingly applied in part design within the modern automotive industry due to their low density and outstanding mechanical properties. Additionally, injection moulding is an economic process to produce parts in large quantities. However, the distribution and orientation of fibres within the components are heavily dependent on the moulding process and the material behaviour is characterised by numerous effects like non-linearity, plasticity and strain-rate as well as temperature dependency. Therefore, it can be considered challenging to predict the mechanical behaviour of parts made of SFRPs by simulation. Meaningful results can only be achieved by coupling an injection moulding and a structural simulation – the so called integrative simulation. To make these integrative simulation methods accessible in early design stages, when a quick estimation of the structural behaviour is required, Gruber and Wartzack developed a simplified approach, called Integrative Simulation 4 Early Design Steps (IS4ED). It considers the material's anisotropy by using the fibre orientation data gained from the injection moulding simulation. By reducing the complexity of the orientation condition and the material representation, a simulation approach suitable for early design stages was created. [1]
However, within the IS4ED-approach the influence of high or low temperatures on material behaviour is not considered. As thermoplastic matrix materials are sensitive to changes in temperature, IS4ED has to be enhanced. The decreases of stiffness and maximum stress levels as well as the increase of maximum strain at elevated temperatures have to be added to the approach. Within automotive applications, structural parts may be exposed to a temperature range from -40 °C up to 100 °C [2]. At these temperatures, the fibre-supporting properties of the thermoplastic matrix material decline, which especially affects compressive loading. Still, occupant safety has to be maintained even at extreme conditions. As it seems likely that anisotropy influences the temperature-dependency, relevant changes to the part can only be taken within the early design stages. Therefore, the basic concept of IS4ED still remains the same.

2 State of the art: The IS4ED approach

The IS4ED approach by Gruber and Wartzack can be divided into two major sub-steps: the determination of the local fibre orientation state within SFRP parts and the definition of a numerical material description.

2.1 Calculation and representation of fibre orientation

As derived by Advani and Tucker, the fibre orientation can be described by a second-order tensor, a_{ij} [3]. While its eigenvectors, e_i, display the direction of fibre distribution, its eigenvalues λ_i indicate the orientation distribution probability. Consequently, the orientation tensor can be visualised as an orientation ellipsoid using the eigenvectors and eigenvalues as shown in fig.1.

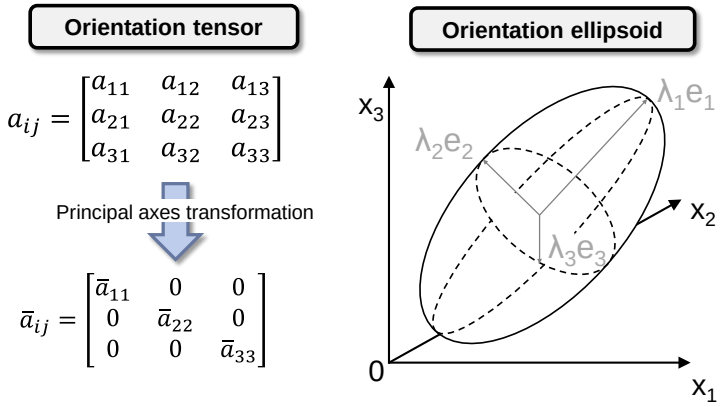

Fig.1: Visualisation of fibre orientation as ellipsoid *[9, 3]*

The fibre orientation tensors are calculated for each node in the injection moulding simulation. While process simulation tools use 3D tetrahedron meshes, 2D quad shell elements are beneficial within crash simulation of thin walled structures. Therefore, the fibre orientation *ellipsoids* with the three semiaxes λ_i have to be averaged and projected onto the shell's surface as orientation *ellipses* with two semiaxes θ_i. This reduction to a 2D fibre orientation state causes a loss of information about the reinforcement orthogonal to the shell surface. This, however, can be tolerated as the normal-oriented fibres provide no reinforcement against loads within the shell plane. In addition to that only a minor percentage of fibres are oriented in normal direction. [4]

2.2 Material description

For structural analyses with the IS4ED approach, shell discretisation is used, as the focussed thin-walled injection-moulded parts can be efficiently represented. The material behaviour of SFRP is modelled by superposition of two material definitions within a finite shell element. A transversal-isotropic and an isotropic, elastic-plastic material description is used. The transversal-isotropic material model, ***MAT_54**, enables the representation of anisotropic stiffness with only a few material parameters. ***MAT_24** or ***MAT_98** are used for describing the elastic-plastic material behaviour. The layer-based superposition of material models is shown in fig.2.

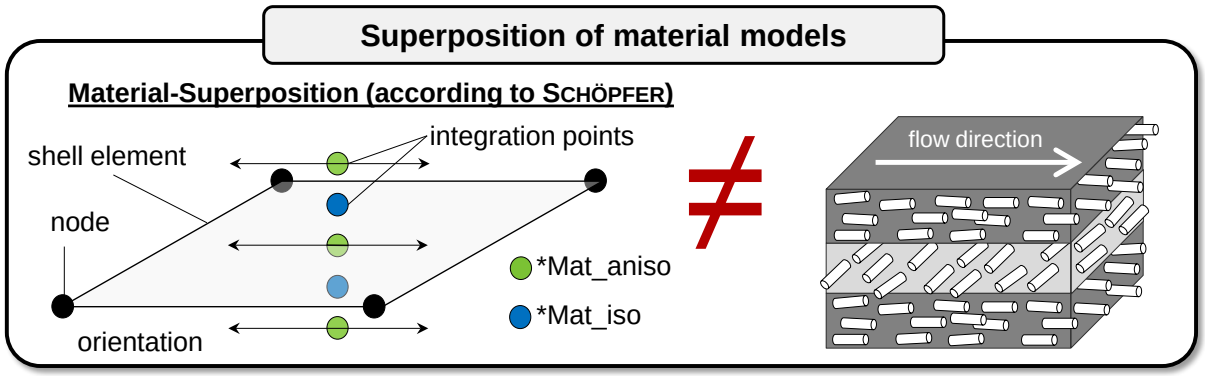

Fig.2: Superposition of material models in shell elements *[2]*

The material models are alternatingly implemented onto the element's through-thickness integration points. This is achieved by using the keyword ***ELEMENT_SHELL_COMPOSITE**, which is commonly used to model laminated composites. Within the IS4ED approach, the single layers do not represent the distinct layers of SFRP. It aims to represent the macroscopic rather than the microscopic material behaviour and therefore the fibre orientation is considered as constant for all layers within a single element. ***ELEMENT_SHELL_COMPOSITE** allows assigning a material model and material angle to each integration point of the element. This way, the orientation information as given from the process simulation can be used in structural analyses. [5]

While strains are constant over all integration points of a shell element, stresses differ due to the varying material models. Consequently, stresses have to be averaged, weighed by their respective layer thickness:

$$\bar{\sigma}_{xx} = \sum_{i=1}^{i=n} \sigma_{xx,i} \cdot \frac{t_i}{t_{total}} \tag{1}$$

where $\bar{\sigma}_{xx}$ is the averaged stress, $\sigma_{xx,i}$ is the stress within the *i*-th layer and t_i or t_{total} are the thickness of the *i*-th layer or all layers' thicknesses summed up. [4]

2.3 Definition of Material Classes

The variation of stiffness and firmness caused by the fibre orientation state is taken into account by introducing material classes. The material parameters calculated by reverse engineering are only valid for areas with a fibre orientation state comparable to the tensile test specimen. Therefore, the material parameters are adapted to the local orientation state. By using material classes, the calculation effort is reduced. The classification depends on the orientation distribution probabilities (ODP). With the equations below, the conditions for the orientation probabilities are displayed.

$$\theta_I \geq \theta_{II} \text{ and } \theta_I + \theta_{II} \leq 1 \tag{2), (3}$$

$$\theta_{II} \leq 0{,}5 \tag{4}$$

The definition of nine material classes is illustrated in fig.3.

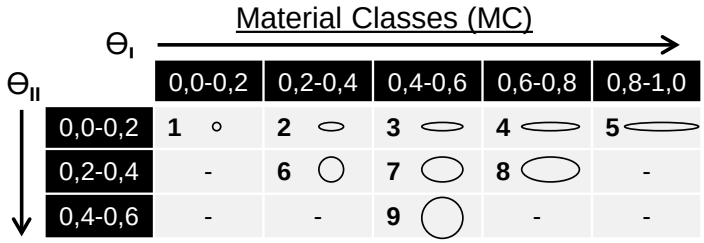

Fig.3: Definition of material classes according to fibre orientation probability [4]

The parameters for the Young's moduli are interpolated regarding the a- and b-direction of the anisotropic material model for each material class. Testing is performed with specimen of ideal orientation, i.e. material class 5.
Consequently, the model for structural analysis contains the following information for each element:

- fibre orientation direction, given as material angle for **`*ELEMENT_SHELL_COMPOSITE`**
- anisotropic stiffness parameters in *a*- and *b*-direction, depending on the fibre orientation probability or material class respectively
- isotropic stiffness parameters
- thicknesses for the anisotropic and isotropic layers.

3 Characterisation of temperature-dependent material behaviour of SFRP

The mechanical material behaviour of short-fibre reinforced plastics with a thermoplastic matrix material is suspect to react sensitively on temperature influences. Generally, an increase of temperature results in a decrease in stiffness and maximum stress and an increase in maximum strain compared to room temperature. A series of quasi-static and high-speed tensile tests is performed with a 20% glass fibre reinforced blend of PBT and ASA at different thermal conditions.

3.1 Testing conditions and test specimen

All tests are performed at a servohydraulic tensile testing machine of the type Zwick/Roell HTM 5020. Displacement and strains are measured optically by Digital Image Correlation with two stereoscopic high-speed cameras and the measurement system GOM ARAMIS HS. The optical measurement enables visualising local strain and strain rate differences. Additionally, not only technical but also true stress can be determined by relating the measured force not to the initial cross section, but to the actually existing. Except for room temperature, all tests are performed within a temperature chamber.

Testing speed is altered between 0.01 and 4 m/s, resulting in effective strain rates from 10 s^{-1} up to 200 s^{-1}, temperature is varied between -20 °C and 100 °C. Temperature can be considered as constant during a test, as the testing time is in a magnitude of only a few milliseconds to seconds. Testing velocity differs from the nominal value during the test. Initially, the hydraulic piston has to be accelerated. During acceleration time, no force may be applied onto the specimen. Instead, specimen are to be loaded only when the nominal testing speed is reached for the piston. Nevertheless, the specimen itself cannot reach the testing speed instantly from idle state. Thus, strain rate increases rapidly at the beginning of the test and covers a wide range of values.
The test specimen according to Becker [6] are taken from an injection moulded, ideally oriented reference plate as shown in fig.4. Thus, stress-strain-curves are determined for parallel (0°) and orthogonal (90°) loading.

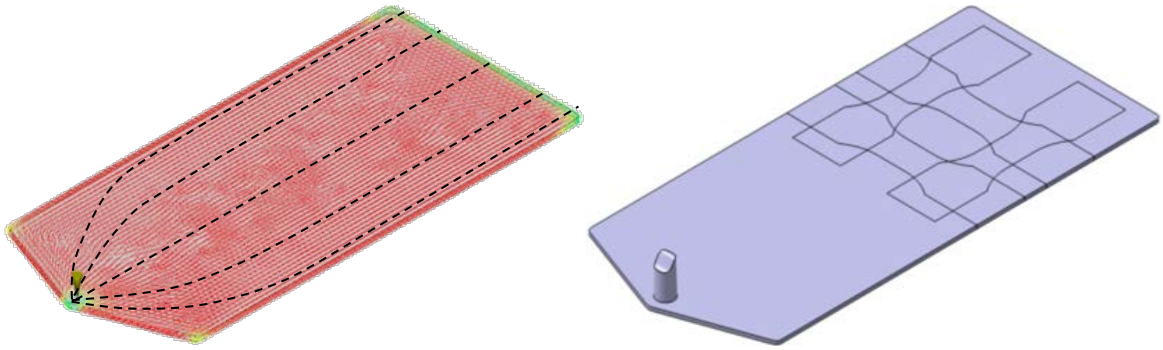

Fig.4: Reference plate with primary orientation direction and specimen location [4]

3.2 Characterisation results

Fig.5 displays the results of tensile tests with varying testing conditions. Plot (a) and (c) display a set of tests performed at the lowest testing speed, 0.01 m/s and at seven temperatures (-20, 0, 23, 40, 60, 80 and 100 °C). Plot (b) and (d) show tests performed at room temperature (23 °C) with four different testing speeds (0.01, 0.5, 2 and 4 m/s) and accordingly, strain rates. The tests for (a) and (b) were performed with orthogonal fibre orientation, (c) and (d) with parallel fibre orientation respectively.
Although plots (b) and (d) are taken from tests with the same nominal velocity, it is conspicuous that the strain rates for all tests with orthogonal fibre orientation are higher than with parallel fibre orientation. Two reasons can be named for that: firstly, the actual piston speed is not constant during the test. Instead, its speed is slightly lower for specimen with parallel fibre orientation as, due to the higher specimen stiffness, the piston is decelerated stronger. Secondly, even with identical piston speed and displacement, the lower stiffness of orthogonally oriented specimen leads to higher strains and thus, higher strain rates. This can be confirmed by virtual tensile tests [4].
The displayed plots contain raw test data. For later use, the raw data has to be edited: The curves need to be averaged over test repetitions and approximated by e.g. polynomic interpolation as it they are required to be monotonically increasing.
For further investigation, the stiffness and failure strain vs. temperature are taken into account. Strain rate does not affect the stiffness of SFRP within the elastic regime and will therefore not be examined in this case [4]. The elastic modulus for later use is calculated as secant modulus between 0 and 1 % strain.

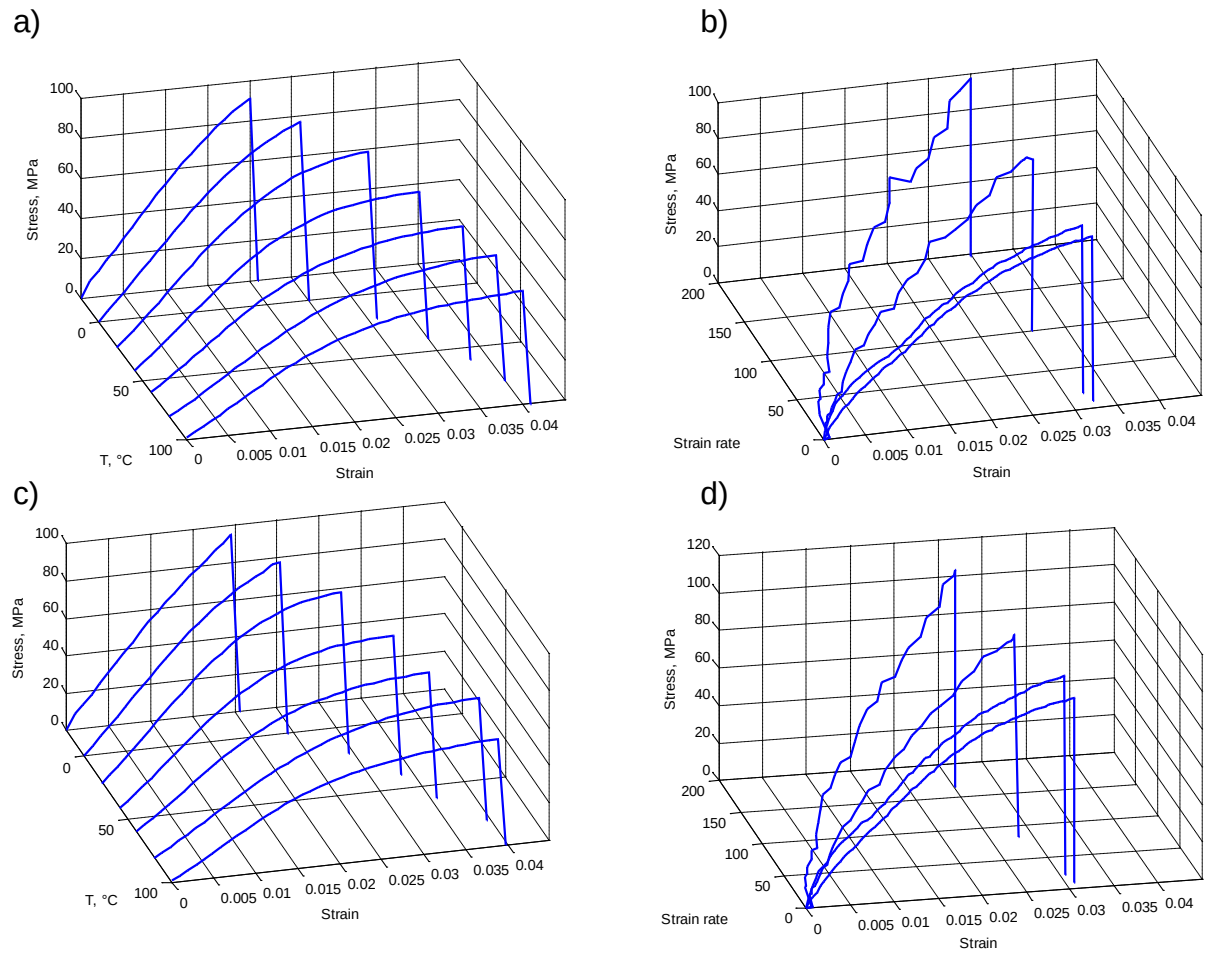

Fig.5: Stress-strain curves over temperature and strain rate

3.2.1 Temperature influence on stiffness

The stress-strain curves measured in the tensile tests suggest a decrease of stiffness with increasing temperature. This is indicated in fig.6, in which the elastic modulus parallel and orthogonal to fibre orientation is displayed over the testing temperature. The results vary between 5.300 MPa (-20 °C) and 1.800 MPa (100 °C) among orthogonal specimen and between 6700 MPa (-20 °C) and 1900 MPa (100 °C) among parallel reinforced specimen. For the later use within simulation, the Young's modulus is saved as a load curve.

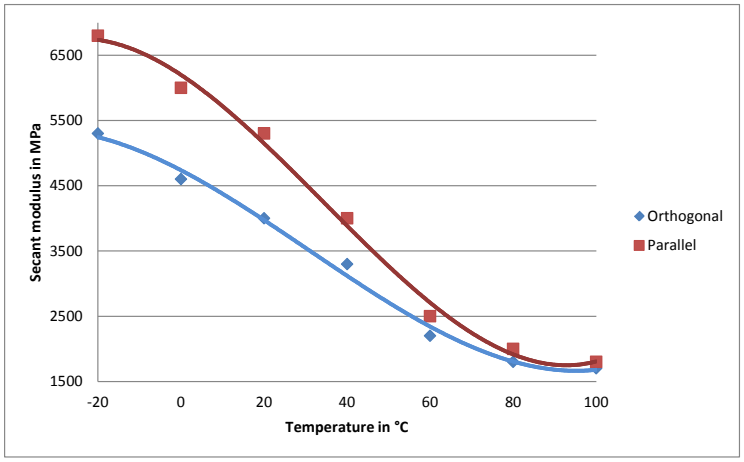

Fig.6: Elastic modulus over temperature

The elastic modulus can be approximated by a polynomic function of temperature. In this case, a cubic function is chosen.

$$P(\mathrm{x}) = \sum_{i=0}^{3} a_i x^i \tag{5}$$

$$E(T) = E(T_0) \cdot \delta_E(T) \text{ with } \delta_E(T) = \frac{P(x=T)}{P(x=T_0)} \tag{6),(7}$$

3.2.2 Temperature influence on failure strain

The failure strain of SFRP increases with temperature. As shown in fig.7, the results of the quasi-static tensile tests vary between failure strains of 2.1 % at a temperature of -20 °C and 4.1 % at a temperature of 100 °C.

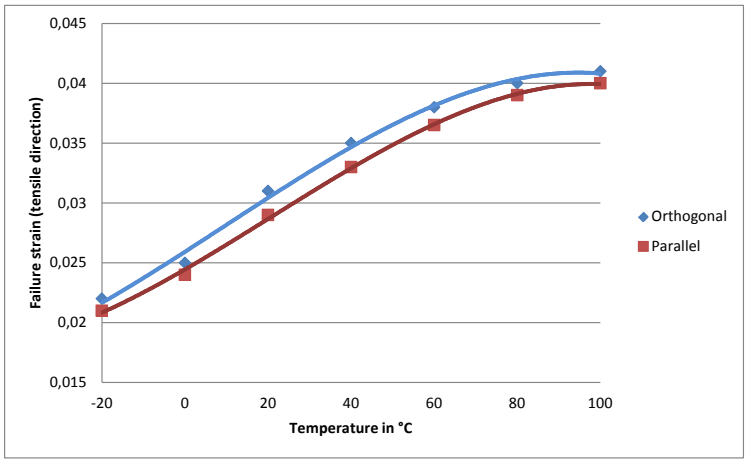

Fig.7: Failure strain of SFRP over temperature

4 Simulative approach: Thermal IS4ED

As described in chapter 3, the mechanical behaviour of SFRP reacts sensitively to changes in temperature as well as in strain rate. Additionally, anisotropy has to be covered within the material description as well. Thus, a set of material models has to be found that is capable of dealing with all effects mentioned. Material model 224, ***MAT_TABULATED_JOHNSON_COOK**, offers the desired characteristics except for anisotropy. Therefore, a layered model using ***MAT_54** and ***MAT_224** will be set up. [7]

***MAT_224** resembles the original Johnson-Cook material model, ***MAT_15**, but with the possibility of tabulated input parameters. The analytical formulations of the Johnson-Cook constitutive model, see (8), are replaced by arbitrarily defined tables. Thus, effective stress versus effective plastic strain curves can be set up as quasi-static for different temperatures as well as isothermal for different strain rates. A temperature dependent, isotropic Young's modulus can be given as curve as well. [3]

$$\sigma_{eff} = \left(a + b\varepsilon_p^n\right)\left(1 + c\ln\left(\frac{\dot{\varepsilon}}{\dot{\varepsilon}_0}\right)\right)\left(1 - \left(\frac{T - T_R}{T_m - T_R}\right)^m\right) \tag{8}$$

where σ_{eff} is the effective stress, ε_p is the effective plastic strain, $\dot{\varepsilon}$ is the strain rate and $\dot{\varepsilon}_0$ is the reference strain rate. Coefficient *a* is the yield strength, *b* is the hardening modulus and *c* is the strain rate sensitivity coefficient. The exponents *n* and *m* describe plastic hardening and thermal softening.

To generate the required data, tables including load curves have to be set up. The procedure will be demonstrated with the variables LCK1 and LCKT from card 2 in ***MAT_224**.

LCKT points to a table ID defining for each temperature value a load curve ID giving the (quasi-static) effective stress versus effective plastic strain for that temperature, LCK1 points to a table ID defining for each plastic strain rate value a load curve ID giving the (isothermal) effective stress versus effective plastic strain for that rate [8]. As the test results span a four-dimensional vector space based

on stress, strain, strain rate and temperature, the required two-dimensional stress-strain curves have to be derived by setting strain rate and temperature as constants.
The test data result in a series of points in space that is used to fit a response surface that creates a continuous relationship between the four dimensions stress, strain, strain rate and temperature [9]. This can be achieved by using the capabilities of LS OPT. Fig.8 shows a three-dimensional response surface plot for stress, strain and strain rate at a constant temperature of 23 °C for orthogonally oriented specimen. Stress vs. strain curves are extracted from the metamodel for constant strain rates of 1 s^{-1} and 100 s^{-1}. These curves can be exported to ASCII as well to generate appropriate curves for ***MAT_224** after cutting off the elastic part of the curve.

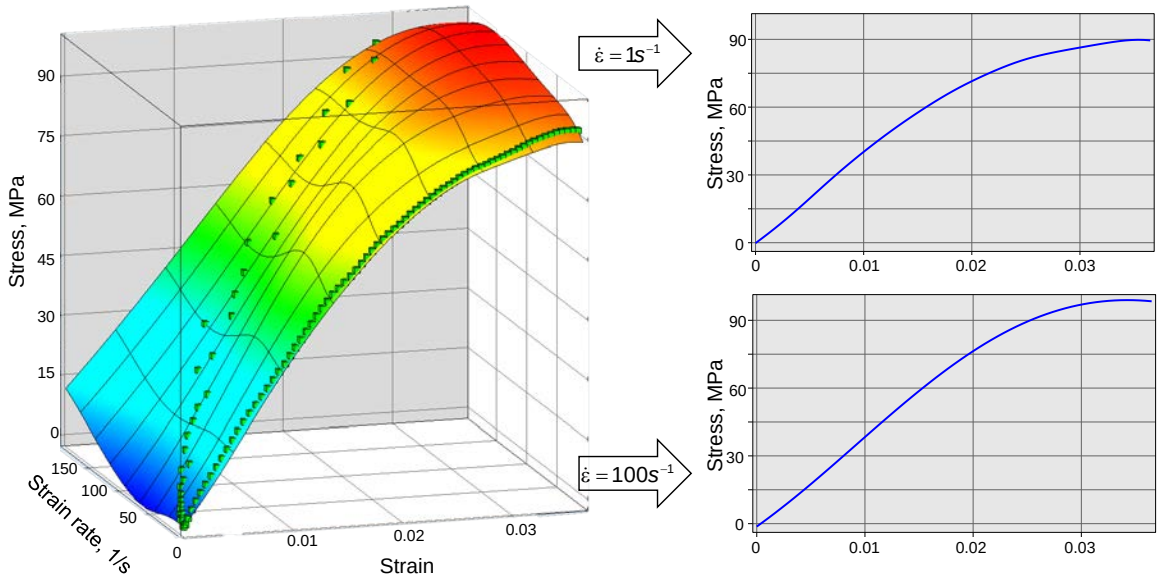

Fig.8: Three-dimensional response surface plot and resulting two-dimensional curves

By using the ***MAT_224** (or also ***MAT_15**) material description instead of ***MAT_98**, the parameter optimisation methods developed for IS4ED can be kept. A virtual tensile test is set up in LS-DYNA and the stress and strain levels in load-direction are compared to actual test results as displayed in fig.9.

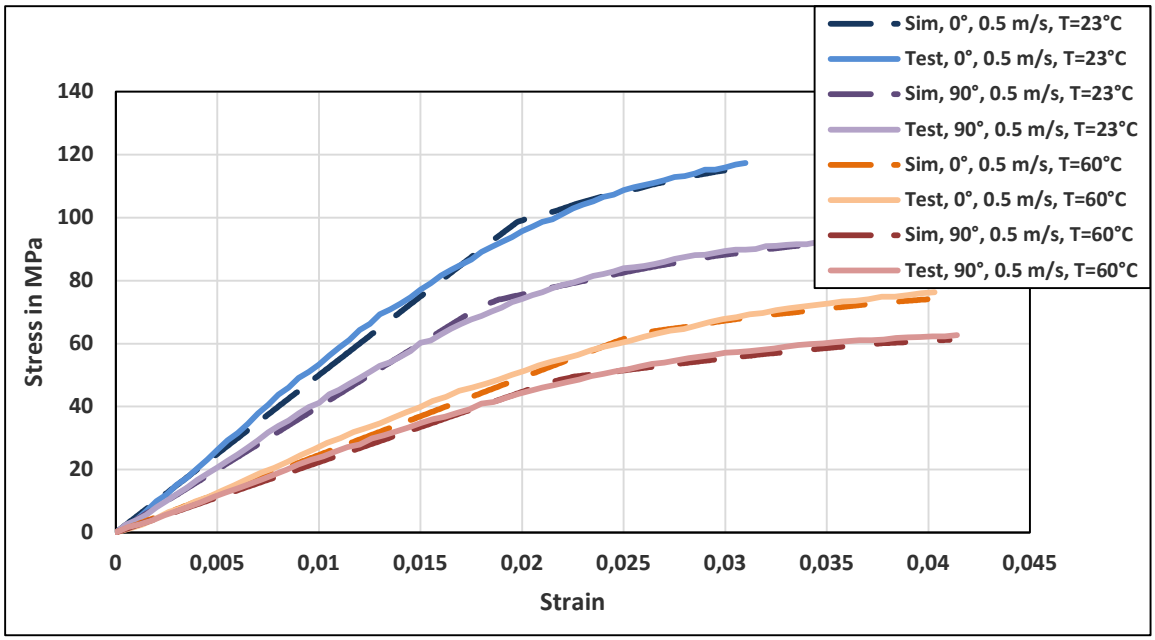

Fig.9: Comparison between test and simulation

The curves show results for tests and simulations at room temperature and 60 °C with a (nominal) loading speed of 0.5 m/s. The simulation results are obtained with ***ELOUT** for a shell element within the center of the virtual test specimen, as it is shown in fig.10, and then averaged over shell thickness integration points.

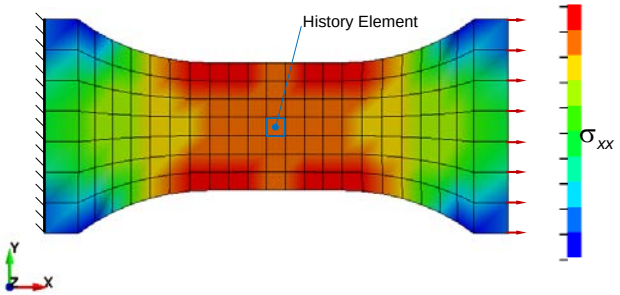

*Fig.10: Virtual test specimen with highlighted ***History_Element_Shell***

5 Summary and perspective

The present paper dealt with the influence of temperature on the mechanical behaviour of short fibre reinforced polymers. A series of tensile tests was carried out within temperatures between -20 °C and 100 °C and with testing speeds from 0.01 m/s and 4 m/s, resulting in strain rates of up to 200 1/s. Test specimen with fibre orientation parallel and orthogonal to load direction were examined. Though they are not affected by differing strain rates, the material's elastic properties are strongly dependent on temperature changes for both parallel and orthogonal fibre orientation.
The original IS4ED approach by Gruber and Wartzack with a layered material description using ***ELEMENT_SHELL_COMPOSITE** with the anisotropic material model ***MAT_54** and the isotropic material model ***MAT_98** is adjusted and the isotropic layers are implemented with ***MAT_224**, a tabulated version of the Johnson-Cook material model. Thus, thermal softening may be applied within the simulation.
After parameter optimisation, simulation and test results are compared. However, no validation experiments such as drop tests could be carried out yet. Performing such experiments will be subject of future work in order to prove the validity of the simulation concept.

6 Literature

[1] Gruber, G.; Wartzack, S.: "Evaluierung der orientierungsbezogenen Leichtbaugüte", Lightweight Design, No. 5/2013, pp. 18-23.
[2] Dehn, A.: "Experimentelle Untersuchung und numerische Simulation des Crashverhaltens gewebeverstärkter Thermoplaste unter Temperatureinfluss". PhD-Thesis, TU Kaiserslautern, 2001.
[3] Advani, S.G.; Tucker C.L.: "The use of tensors to describe and predict fiber orientation in short fiber composites". Journal of Rheology, 31(8), 1987, pp. 751-784.
[4] Gruber, G.: "Ein Beitrag zur rechnerunterstützten Auslegung crashrelevanter kurzfaserverstärkter Kunststoffbauteile in der frühen Entwurfsphase", PhD-Thesis, University of Erlangen-Nuremberg, 2014.
[5] Stelzmann, U.; Hörmann, M.: "Ply-based composite modelling with the new *ELEMENT_SHELL_COMPOSITE keyword". In: Tagungsband zur 8. Europäischen LS-Dyna User's Conference. Strasbourg, 2011.
[6] Becker, F.: "Entwicklung einer Beschreibungsmethodik für das mechanische Verhalten unverstärkter Thermoplaste bei hohen Deformationsgeschwindigkeiten". PhD-Thesis, Martin-Luther-Universität Halle-Wittenberg, 2009.
[7] Gilat, A.: "Development of Deformation and Failure Model (MAT 224) in the LS-DYNA Finite Element Program". International Symposium on Current Problems in Solid Mechanics. Symi, 2012.
[8] Livermore Software Technology Corporation (LSTC): "LS-Dyna Keyword User's Manual", Version 971 R 7.1; Livermore, USA, 2014.
[9] Witkowski, K. et al.: "New Features in D-SPEX with Application". In: Tagungsband zum 6. LS-DYNA Anwenderforum, Frankenthal, 2007.